Science Forum (Journal of Pure and Applied Sciences)

journal homepage: https://atbu.edu.ng/science-forum/

Petrography, morphology, and geochemistry of migmatites around Dungal, Bauchi North East Nigeria

Amina Ali[1], Ahmed Isah Haruna[2], Abdulmajid Isa Jibrin[2*], Faisal Abdullahi[2], Tahir Garba[2]

[1] *National Center for Petroleum Research and Development, Bauchi, Nigeria*

[2] *Abubakar Tafawa Balewa University, Bauchi, Nigeria*

ABSTRACT

The general geology of rocks around Dungal was accessed with a view to classify the rocks and determined their tectonic origin using field relationship, petrography and geochemistry of the rocks. The rocks were classified as migmatite which were further sub divided into metatexite, diatexite, and pegmatitic neosome. Geochemistry indicates that they are formed from mixtures of magmas, addition or subtraction of solid phases by contamination or fractional/partial melt crystallization. They are peraluminous and calc alkaline affinity which indicates that they from metasedimentary sources, also the high content of SiO_2 ($Na_2O + K_2O$) and Al_2O_3, MgO, Fe_2O_3, & CaO low concentration imply that the magma was derived from partial melting of the lower crustal rocks.

ARTICLE INFO

Artcle history:
Received 12 February 2023
Received in revised form
11 February 2023
Accepted 12 February 2023
Published 06 July 2023
Available online 06 July 2023

KEYWORDS

Morphology
Migmatite
Dungal
Metatexite
Diatexit

1. Introduction

Dungel and environs forms part of the Nigerian Basement complex of Bauchi area (Fig. 1) which forms part of the Neoproterozoic Trans-Saharan belt formed between 700 and 580 Ma by accretion of terranes between the converging West African Craton, the Congo Craton, and the East Saharan Block (Ferre and Caby, 2006). The geology of the area is characterized by metamorphic rocks of Neoproterozoic which are termed as Pan-African Granitoids (Older granite) and associated younger granitic rocks (Fig. 2). These rocks are mostly migmatite, bauchite (Charnockite), and other granitic rock that made up the geologic suite (Fig. 2b). The rock in the study area are characterized by metamorphic features such as magmatic foliation, mineral lineation which are due to the effect of partial melting. The deformed features of the rocks around the study area necessitated the study in order to unravel the geology of the study area using the recent state of art multi-disciplinary research on migmatite (morphology).

2. Regional Geology

Nigeria is located within the mobile belt which separates the West African Craton to the west from the Craton to the south east. According to Ajibade and Fitches (1988), Ajibade and Rahaman (1988), this mobile belt was affected extensively by the widespread pan- Africa thermo tectonic event of 600 ± 150 ma but relies of the ovular rocks dating to Archean (3,500 ma) as well as lower proterozoic (2,000 ma) can still be found in the Nigerian basement complex. The complex structures and Geochronological relationship among basement rocks provide much of the

* **Corresponding author** Abdulmajid Isa Jibrin ✉ aali@ncprd.atbu.edu.ng ✉ Abubakar Tafawa Balewa University, Bauchi, Nigeria.

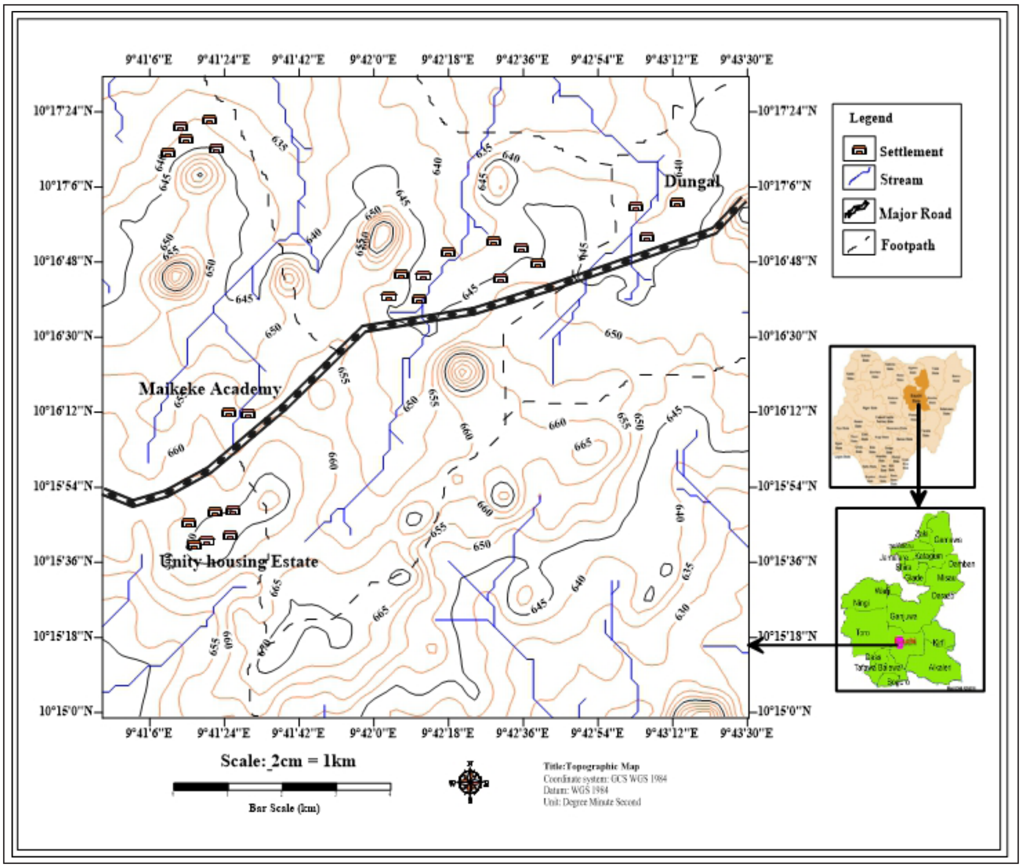

Figure 1. Location map of the study area.

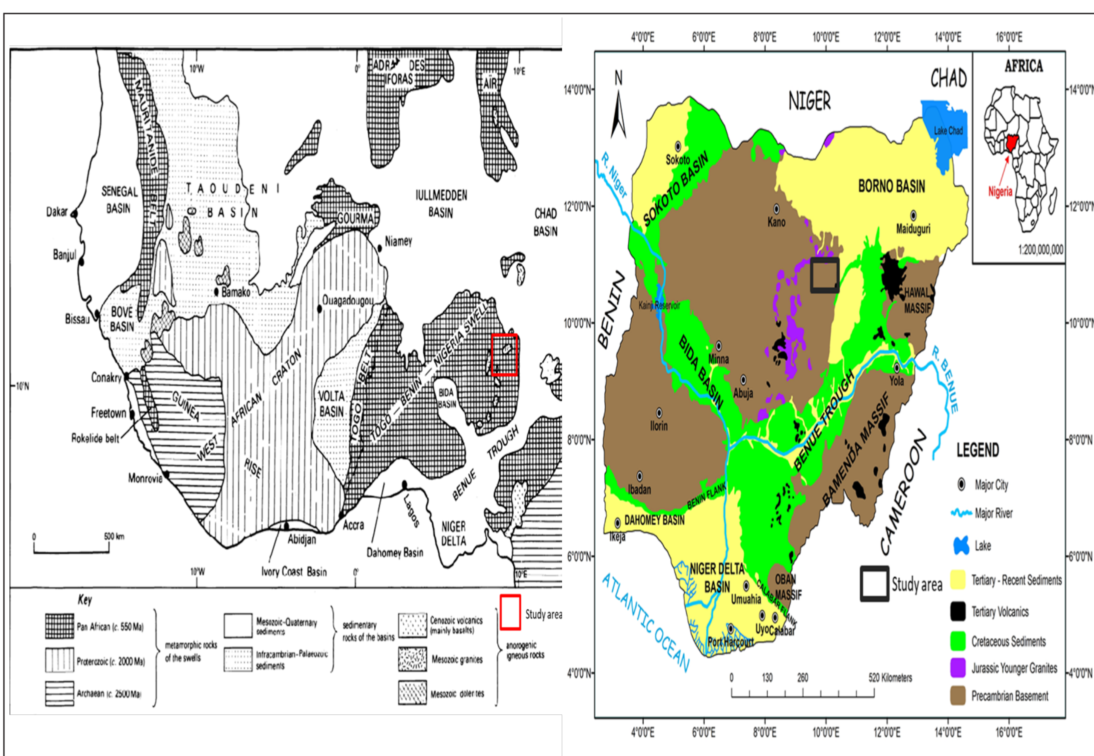

Figure 2. Location map of the study area (modified from Jibrin et al., 2018).

evidence for crystal reactivation i.e. the Basement is made up of rocks that have experienced the effect of more than one thermo-tectonic event (Wright, 1985; Wright et al., 1985). Rocks of elongated supracrustal belts occupy synclinorial structure within the basement, which have a varied lithology and mineralogy and represent sediments and volcanic of many different types. These rocks are called supracrustal because they look as though they were originally deposited upon the basement and are therefore younger (Collins et al., 1982).

Their contact relationships with Basement rocks are commonly gradational or sheared due to faulting or thrusting (where exposed) and direct evidence of superpositions is rare (Hirsh et al., 2002).

Syn-tectonic to late tectonic plutonic intrusion are mainly of Granite to Granodiorite in composition, but include smaller masses of Diorite, Gabbro, Syenite, and related rocks. They intruded both basement and supracrustal. Contacts with basement rocks vary from concordant and gradational to sharp and cross-cutting. Their filed and chronological relationship indicates that emplacements occurred during the last of the reactivation event that affect the Basement. i.e during deformation and metamorphism of the supra-crustal (Wright et al., 1985). The major factor that controls the transformation of Bauchi rocks from metatexite migmatite to diatexite migmatite and subsequently to leucogranites is partial melting or liquid absent melting (Jibrin et al., 2021).

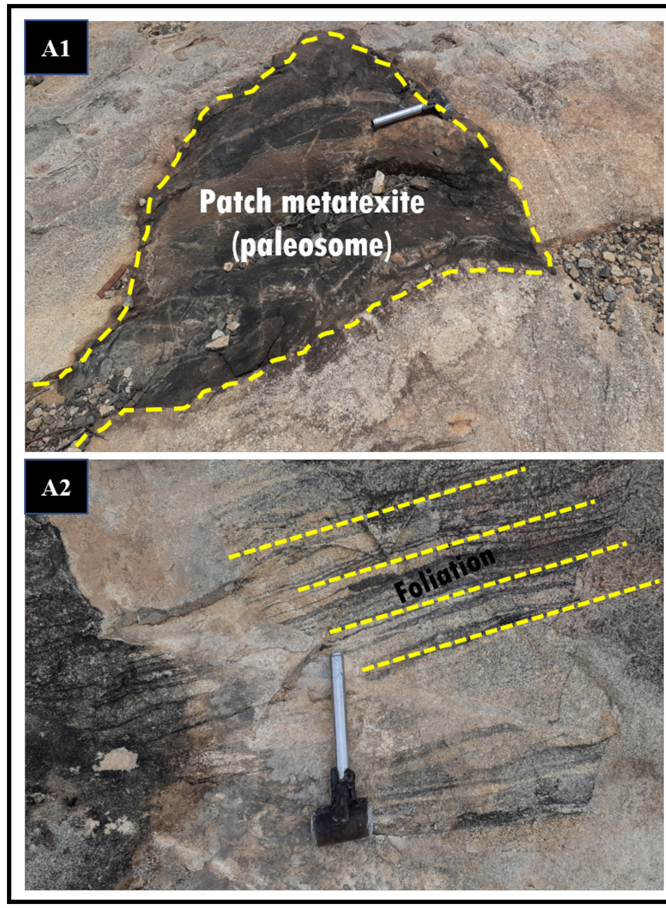

Plate 1. Field photograph showing metatexite. (A1) patch metatexite (A2) metatexite occupying foliation planes within diatexite.

3. Results and Discussion

Field work was conducted in order to ascertain and classify the different rock type and their field relationship. A total of 21 representative samples were collected for petrographic and geochemical analysis. Petrographic analysis was conducted at petrographic laboratory Abubakar Tafawa Balewa University Bauchi while the geochemical analysis was done at National Geoscience Research laboratory Kaduna Nigeria. Based on micro, microscopic, geochemistry, field relationship, structures identified in the field and other regional evidences the rocks were classified as migmatites which were grouped into metatexite, diatexite and nebulitic migmatite.

3.1. Metatexites

The metatexite in the study is patch to stromatic showing evidence of foliation. They are banded by discontinuous millimetric to centimetre thin layer of medium grained quartz and plagioclase leucosomes alternating with centimetric melanosomes (Plate 1). They are concordant to local foliation. Metatexite in the diatexites show a darker coloration and high paleosome ratio of residual composition, which shows an evidence of passive enrichment in residual minerals after the melt removal. Gradational contact between the with stromatic and sharp contact with paleosome was encountered

A representative sample of metatexite obtained was described in terms of its texture, color, and possible mineral visible under hand lens, a fresh sample is dark in color and medium grained in texture, foliations (Schistosity), the metatexite are defined by alignment of platy minerals (Plate 2). The modal analysis of metatexite and other metamorphic minerals is shown in Plates 1–4.

Minerals identified using transmitted light microscope in plane polarized light (PPL) and cross polarized light (XPL) mode exhibited the following properties; quartz is colorless, non-pleochroic, subhedral in shape and exhibits undulatory extinction, low relief and grey interference color biotite which define the

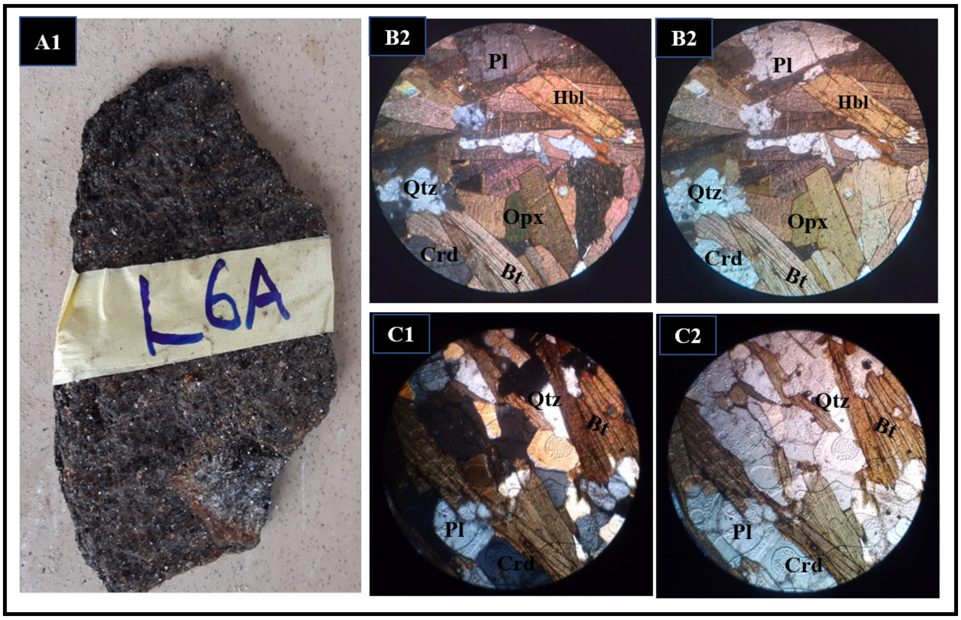

Plate 2. (A1) Hand specimen photograph of metatexite samples, photomicrograph of metatexite samples under cross polarized light (B1 and C1) and PPL (B2 and C2) Q = Quartz, B = Biotite, Opx = Orthopyroxene, Mu = Muscovite, P = Plagioclase.

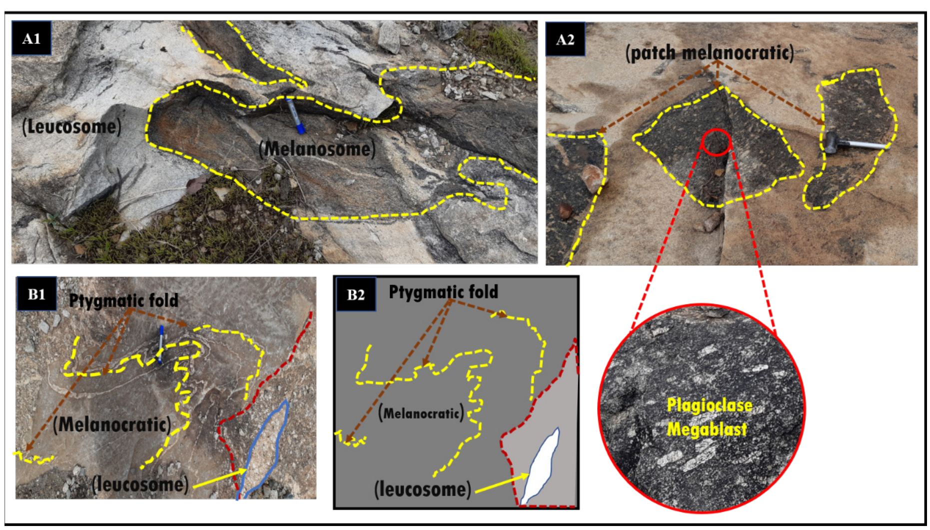

Plate 3. Field photographs showing several aspects of melanocratic diatexites. (A1) melanosome in vicinity of leucosome (A2) melanocratic diatexite with plagioclase megacryst (B1) ptygmatitic fold in melanocratic diatexite and lense of leucosome (B2) schematic description of B1.

foliation shows changes one directional cleavage, brown to dark brown pleochroism and extinction is parallel (Plate 2B1). in both planes polarize and cross.

3.2. Diatexite

3.2.1. Melanocratic diatexite

They are medium grained in texture and occur in vicinity of leucocratic morphologies almost in the study area. It is believed to have been partially migmatized by the intrusion of acidic magma resulting into distinct felsic and mafic bands. The common structure observed in this rock is ptygmatitic folding (Plate 3B2). The patch of the melanocratic diatexite shows megacryst of plagioclase within the ground mass of biotite. The boundary between the melanocratic and leucocratic diatexite is sharp by color differences with

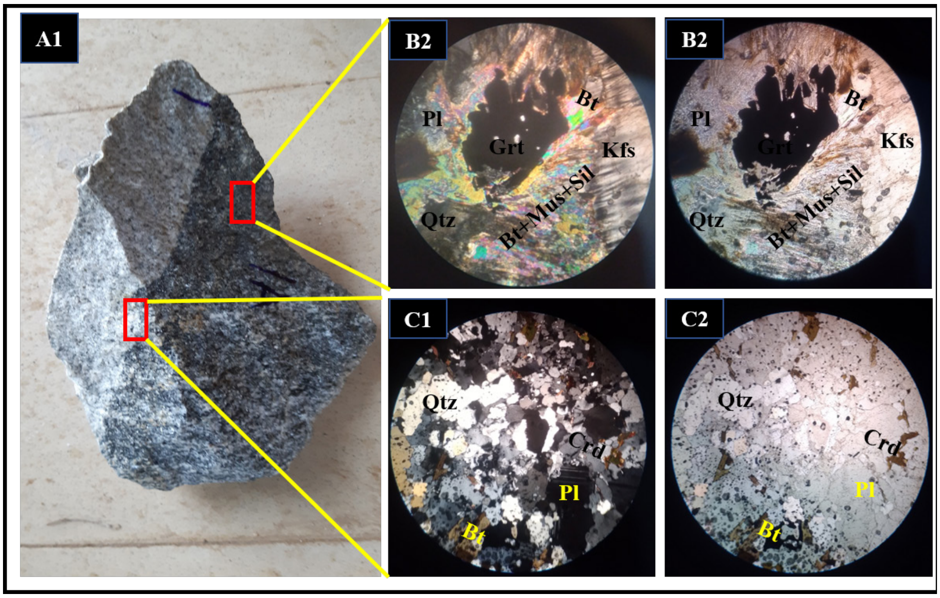

Plate 4. Hand specimen photograph of melanocratic diatexite samples, photomicrograph of melanocratic diatexite samples under cross polarized light (B1 and C1) and PPL (B2 and C2) Q=Quartz, B=Biotite, Opx= Orthopyroxene, Mu= Muscovite, P= Plagioclase.

sharp contact. The plagioclase occurs as megacrystals in the matrix, they are well developed and elongated due to stress (Plate 3A2). The boundary between diatexite and charnockite is also gradational.

Hand description studies revealed that the melanosome (mafic part) consist of biotite and garnet while the leucosome (felsic part) consist of plagioclase, quartz and they shows medium textural architecture (**Plate 4A1**).

3.3. Mesocratic diatexite

Outcrop of this rock was observed within the study area as schlieren and sometimes as body of rock. The outcrop of this form of morphologies appears moderately dark due to high content of ferromagnesian minerals like biotite. The rock is generally poorly exposed. It is medium grained in texture. Field view section study shows that the major mineral present include; quartz, orthoclase, plagioclase and biotite (Plate 5).

It shows a medium grained texture bounded by millimetric foliation, having an almost equal amount of felsic and mafic mineral (**Plate 6A1**). However, minerals that were identified in hand specimens include feldspar, quartz and biotite.

3.4. Leucocratic diatexite

This rock occurs the as granite with foliation plane. It is coarse grained in texture showing a leucocratic appearance in color therefore exhibit it morphological name (Plate 7). The rock is fresh sample could not be obtained for petrographic study. However, minerals that were identified in hand specimens include feldspar, quartz and biotite. The rock at outcrop view split into layer parallel to the foliation plane.

Fresh sample of the leucocratic diatexite obtained was described in terms of its texture, color, and petrographic analysis. It is light in color (Leucocratic). Feldspar formed the crystals with biotite and quartz constituting the groundmass. Its shows medium grain texture and are whitish to grayish coloration (Plate 8).

ken and aligned for two-column display unless sp Minerals identified using transmitted light microscope in PPL and cross polarized light (XPL) mode exhibited the following properties; Quartz is colorless, euhedral in shape, undergo undulous extinction (polycrystalline). Orthoclase is anhedral to subhedral crystal, colorless with no relief in PPL. It occurs as dark grey and a simple twinning in cross polarized light. Plagioclase is colorless, cleavage is perfect, non-pleochroic (Tables 1 and 2), low relief and interference color (grey-white), with parallel extinction. Biotite; brown in color, pleochroic with perfect cleavage, moderate relief, interference color of grey-brown- red- blue-green. (Plate 8B and C).

3.5. Geochemistry

The geochemistry of the samples is presented in Tables 1 and 2 and Harker variation diagrams are used to understand the processes occurring during the evolution of magma. The correlation patterns between

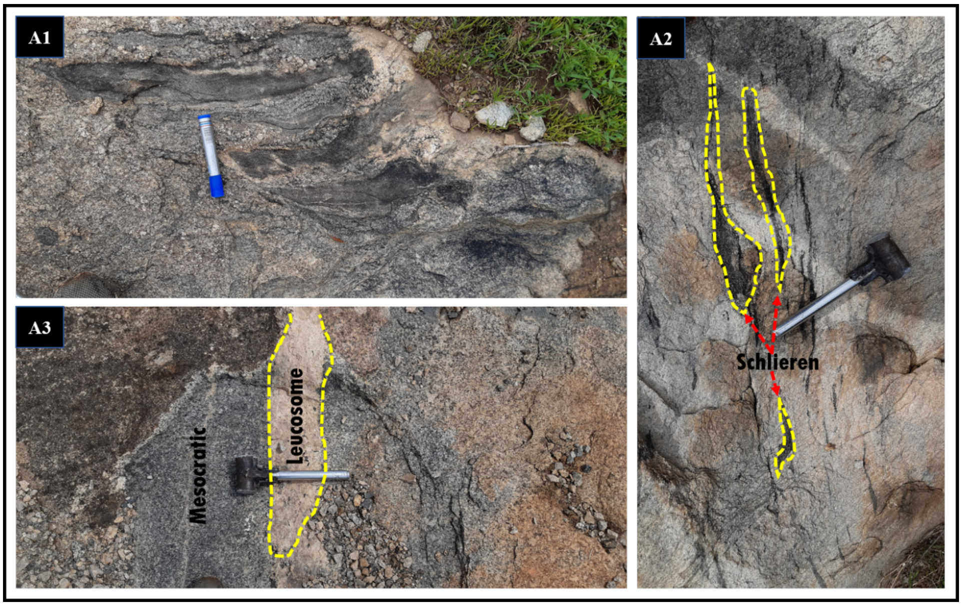

Plate 5. Field photographs showing several aspects of mesocratic diatexites showing schlieritic behaviour and evidence of deformation.

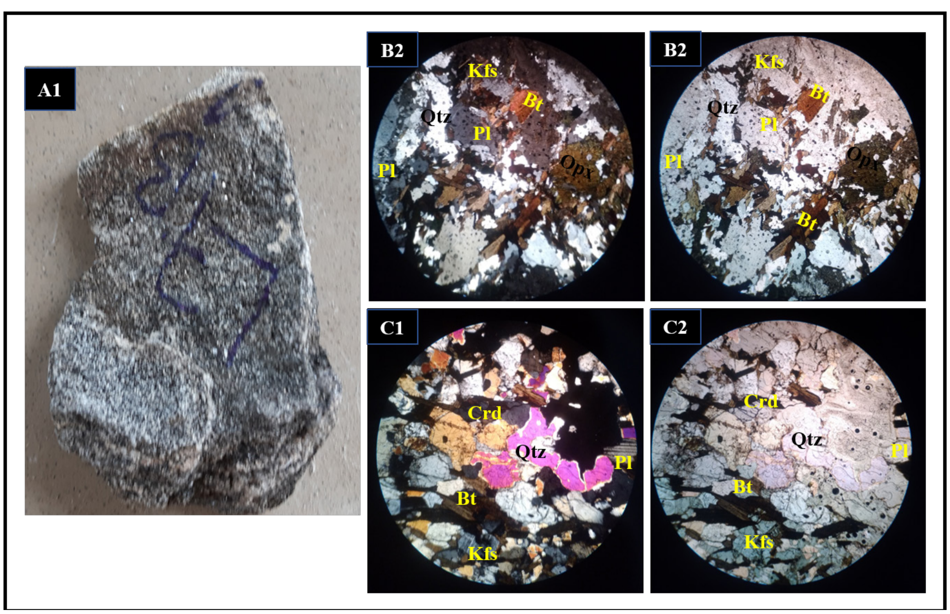

Plate 6. (A1) Hand specimen photograph of mesocratic diatexite samples, photomicrograph of mesocratic diatexite samples under cross polarized light (B1 and C1) and PPL (B2 and C2) Q=Quartz, B=Biotite, Opx = Orthopyroxene, Mu= Muscovite, P= Plagioclase.

selected elements provide an indication in this regard since they are generally related to mixtures of magmas, addition or subtraction of solid phases by contamination or fractional/partial melt crystallization.

Figure 3 shows the projection of major and selected trace elements vs SiO_2 for metatexite, diatexites and pegmatitic neosome.

The B-A diagram as proposed by Debon and Le Fort (1983) with classification fields for various types of peraluminous rocks designed by Villaseca et al. (1998)

(Fig. 4). The B = Fe + Mg + Ti parameter reflects the content of mafic minerals and the A = Al – (K + Na + 2Ca) parameter reflects the amount of aluminium incorporated into feldspars (calculations are based on millications). All the rocks under study (metatexite, and diatexites) fall within the high peraluminous with

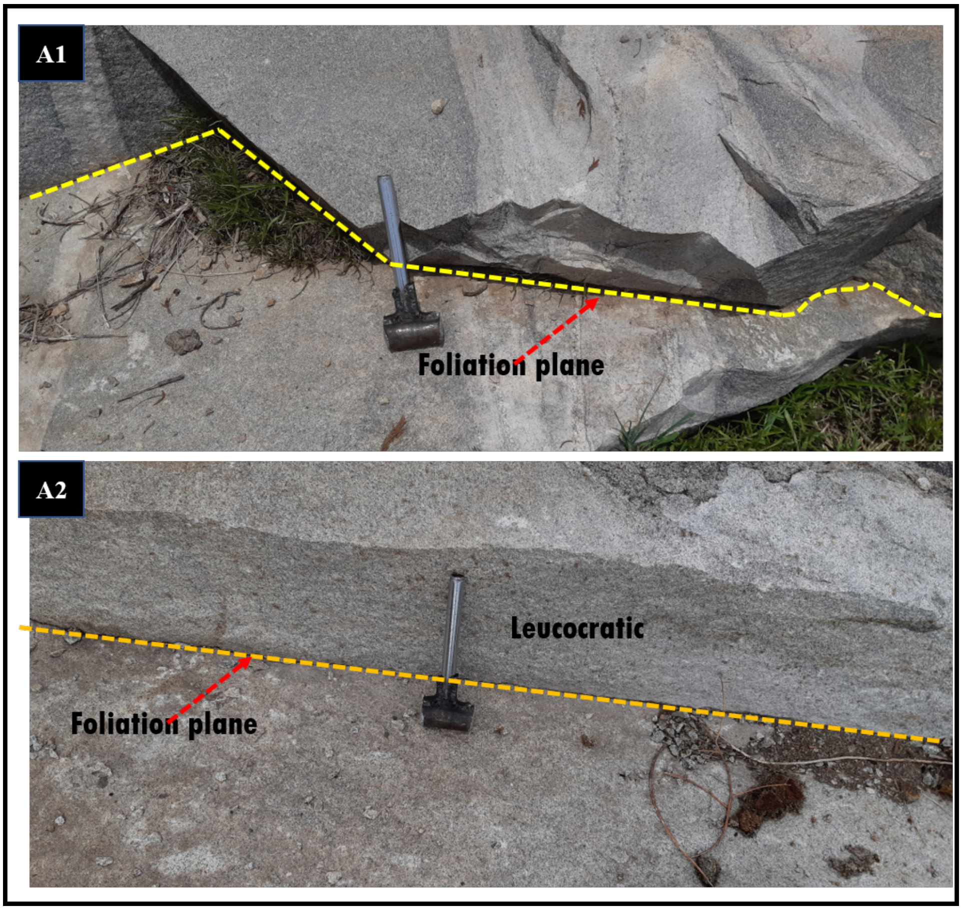

Plate 7. Field photographs showing several aspects of leucocratic diatexites. Showing foliation plane is an evidence for deformation, as inherited from the protolith.

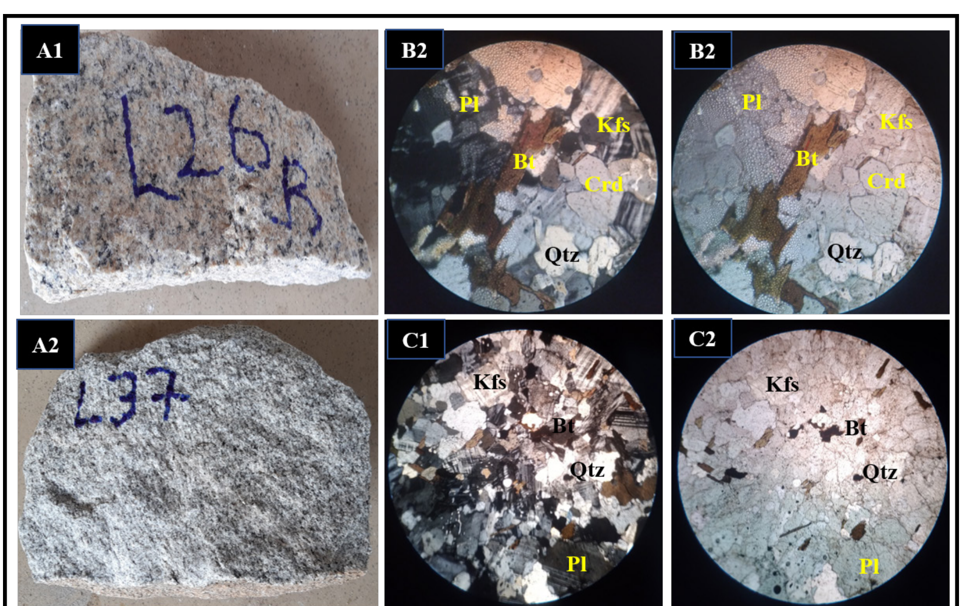

Plate 8. (A1) Hand specimen photograph of leucoocratic diatexite samples, photomicrograph of leucoocratic diatexite samples under cross polarized light (B1 and C1) and PPL (B2 and C2) Q = Quartz, B = Biotite, Opx = Orthopyroxene, Mu = Muscovite, P = Plagioclase.

Table 1. Whole-rock composition [X-ray fluorescence (XRF)], of metatexite, melanocratic diatexite and mesocratic diatexite.

Sample ID	L1a	L1	L2	L4	L5	L6	L7	L9	L8	L10	
Major Element	Metatexite		Diatexites								
SiO2		56.06	56.14	68.3	71.16	72	72	73.4	73.76	73.81	74.1
CaO		0.6	0.52	0.3	0.83	0.2	0.26	0.26	0.08	0.36	0.31
MgO		0.2	0.12	0.1	0.38	0.08	0.12	0.1	0.01	0.17	0.2
SO3		0.07	0.08	Nd	0.01	Nd	0	0	Nd	0	0
K2O		2.6	0.86	8.4	1.28	5.06	4.24	1.12	4.03	5.73	2.68
Na2O		1.84	2.01	1.7	0.63	1.68	1.34	2.68	2	1.06	1.84
TiO2		0.81	1.42	0.21	1.3	0.73	0.26	0.32	0.26	0.08	0.08
MnO		0.03	0.06	Nd	0.03	0.01	0.02	0.04	0.03	Nd	0.01
P2O5		0	0.12	Nd	0.08	Nd	0	0	Nd	Nd	Nd
Fe2O3		18.34	20.46	4.3	5.6	4.35	6.48	7.17	3.6	3.84	4.04
Al2O3		12.46	12.8	13.3	14.34	12.61	13.16	13.42	13.34	13.73	13.63
H2O+		4.88	4.96	2.72	3.03	2.28	1.63	1.36	2.03	1.38	1.89
					Trace Element ppm						
V		480	499.16	825	502	518	416	920	728	740	294
Cr		813.1	780.1	318.02	425	945	560.19	402.06	232.02	237.02	548.29
Cu		449	482	425	1295	330	344	244	435	430	333
Sr		1512	1230	2030	1290	2030	1470	1690	2330	2400	1520
Zr		7350	7140	1780	1720	1500	1600	2040	1650	1690	1240
Ba		1049	1031	650	1000	1800	930	1040	700	730	310
Zn		1230	1320	58.3	52	560	40	480	59	60	27
Ce		80	79	58.13	45.66	54	52	20	61.03	59.08	40
Pb		54	68	94.6	17.9	867	35	25.99	91.3	91	29
Bi		2.13	2.08	0.35	0.21	0.87	0.79	10	0.65	0.66	0.2
Ga		32	33	26.6	17.6	22	32	4	27	26	34
As		3	4	14.05	7.8	17	25	4.08	19.05	15.08	27.02
Y		67	63	2.2	39.7	3.9	35	19	2.9	2.4	25
Ir		5.5	5.7	3.06	3.12	6.09	4.1	4.6	2.1	2.06	2
Au		0.04	0.04	0.73	0.02	0.49	0.42	1.9	0.53	0.51	0.28
Ni		0.02	0.02	<0.001	<0.001	<0.001	0.01	<0.001	<0.001	0	<0.001
Rb		15	14	39.5	9.54	30	17	47	39.8	40	29
Mo		0.01	0.01	<0.001	0.05	0.2	0.01	0.01	<0.001	0	<0.001
Co		1.1	1.2	5.6	<0.001	1.09	1	0.03	5	5.1	0.03
Cd		<0.001	<0.001	<0.001	<0.001	<0.001	0	<0.001	<0.001	0	0.01
Ru		4.32	4.4	8.65	0.42	2.06	1.26	0.98	8.72	8.63	0.12
Eu		24	25	30	126	36	120	33	40	38.9	180
Re		0.01	0.01	<0.001	<0.001	0.05	0	<0.001	<0.001	<0.001	<0.001
Nb		11.6	11.4	17	14.2	83	48	20	19	18.61	32.01
Ag		1.6	1.4	1.5	0.87	0.09	1.12	0.48	1.25	1.4	0.41
Ta		40.54	41	45.2	63	64	36	15	41.2	41.2	42,10
W		12.38	12.31	0.78	13.7	1.46	0.96	2.45	0.88	0.88	0.89
Hf		18.1	18.21	11.2	16.4	21	20	9.09	11	11	33

Continued

Sample ID	L1a	L1	L2	L4	L5	L6	L7	L9	L8	L10	
Yb		0.42	0.46	5.4	1.86	6.9	2.11	2.31	5.9	5.9	4.04
In		4.16	4.2	8.1	3.2	0.09	1.9	1.8	8	8	2.1
Se		0.09	0.11	<0.001	0.38	0.01	0.21	<0.001	<0.001	<0.001	<0.001
U		<0.001	0	<0.001	<0.001	0.01	0.02	0.04	<0.001	<0.001	<0.001
Th		1.03	0.03	0.3	0.76	2.2	1.86	0.18	0.2	0.2	2.58
Sb		9	10.1	4.24	12.5	14	5.13	1.08	3.24	3.24	17.03
Ge		2.06	3.06	68.4	4.1	40	24	4.4	68	68	210
Sn		38.75	35.55	46.4	9.48	20.12	37.33	21.87	43.4	43.4	35.86

Table 2. Whole-rock composition (XRF), of metatexite, melanocratic diatexite and mesocratic diatexite.

Sample ID	L33	L37	L33	L37	L2A1	L3B	L22B	L23	L25	L26B	L32	
Major Element	Diatexite											
SiO2		76.6	76.82	76.6	76.82	70.2	70.3	74.4	74.3	74.81	75.5 75.6	
CaO	0.32	0.21	0.32	0.21	0.02	0.31	0.42	0.43	0.38	0.32 0.19		
MgO	0.15	0.16	0.15	0.16	Nd	0.11	0.2	0.13	0.16	0.08 0.07		
SO3	0.01	0	0.01	0	Nd	Nd	Nd	0	Nd	Nd	Nd	
K2O		1.4	1.3	1.4	1.3	10.4	11.34	1.01	1.8	3.43	4.3 3.63	
Na2O		2.6	2.04	2.6	2.04	1.43	1.4	1.96	1	1.73	1.34 1.06	
TiO2		0.08	0.06	0.08	0.06	0.01	0.04	0.08	0.07	0.12	0.08 0.07	
MnO		0	0	0	0	0.06	Nd	0.01	0.01	0.01	Nd 0.01	
P2O5		Nd	Nd	Nd	Nd	Nd	Nd	0	Nd	Nd	Nd	Nd
Fe2O3		2.51	2.4	2.51	2.4	1.06	3.01	5.72	4.11	3.68	5.01	4.3
Al2O3		13.5	13.52	13.5	13.52	12.08	12.3	13.81	14.88	14.11	13.4 13.58	
H2O+		1.54	1.72	1.54	1.72	2.62	2	1.58	1.74	1.29	1.36	1.7
					Trace Element ppm							
V		759	423	759	423	520	830	641	254	620	410	512
Cr		362.87	260.4	362.87	260.4	670.4	247	352.12	648.29	606	530.34	429
Cu		181	290	181	290	282	362	435	330	383	350	296
Sr		2110	1040	2110	1040	1290	1293	2130	1220	1880	1460 1290	
Zr		1730	1010	1730	1010	1030	2720	1710	1200	1240	1120 1720	
Ba		930.88	680	930.88	680	660	840	700	3100	2110	956	500
Zn		20	150	20	150	180	180	227	97	370	40	30
Ce		54	60	54	60	80	39.88	38.03	50	63	48	65
Pb		72..88	540	72..88	540	68	32	74	26	58.09	30	27
Bi		0.66	3.08	0.66	3.08	3.98	0.15	0.41	0.1	5	0.69 0.22	

Continued

Sample ID	L33	L37	L33	L37	L2A1	L3B	L22B	L23	L25	L26B	L32	
Ga		12	16	12	16	6	9	36	39	5.09	42 27.4	
As		21	10.46	21	10.46	0.46	6	15.65	7.02	3	15.6	37
Y		24	26.7	24	26.7	26	20	2.3	15	4.3	16	29
Ir		28	3.3	28	3.3	3.8	1	2.26	20	2.02	4.1	2.1
Au		0.8	1.68	0.8	1.68	1.6	0.37	0.63	0.22	0.2	0.52 0.31	
Ni	<0.001	0	<0.001	0	<0.001	<0.001	<0.001	<0.001	<0.001	0.08 <0.001		
Rb	27	65	27	65	62	86	29	29	36	41 19.84		
Mo	<0.001	0.01	<0.001	0.01	0.01	0	0.04	<0.001	0.01	0.01 0.01		
Co	1	0.06	1	0.06	1	0.35	<0.001	0.03	<0.001	1.07	<0.001	
Cd	0	<0.001	0	<0.001	<0.001	<0.001	0.5	0.01	0.01	0	<0.001	
Ru	5.07	0.48	5.07	0.48	0.98	8.7	<0.001	0.12	1.23	1.16	0.82	
Eu	57	13	57	13	23	30	0.16	180	34	123	120	
Re	0.01	0	0.01	0	0	0	0.2	<0.001	<0.001	0	<0.001	
Nb	10	60	10	60	60	24.09	24	32.01	42	48.7	14	
Ag	0.87	0.12	0.87	0.12	1.1	0.3	1.03	0.41	0.5	1.32	0.67	
Ta	38	100	38	100	101	64.09	41.2	42,10	55	36.5	64	
W	7.84	8.62	7.84	8.62	5.62	3.99	3.88	0.89	5.06	2.96	13.3	
Hf	6.62	18	6.62	18	28	14	10	33	24	20.5	16	
Yb	2.04	0.29	2.04	0.29	0.19	0.96	1.9	4.04	0.46	3.11	1.76	
In	3.5	2.6	3.5	2.6	2.8	5.2	8.1	2.1	2.23	1.94	3	
Se	0.1	0.12	0.1	0.12	0.22	0.25	<0.001	<0.001	0.28	0.51	0.28	
U	0.1	0.04	0.1	0.04	0.03	0.21	<0.001	<0.001	<0.001	0.03	0	
Th	0.24	0.09	0.24	0.09	0.09	0.22	0.25	2.5	0.31	0.88	1.56	
Sb	0.55	2.14	0.55	2.14	2.24	0.3	3.24	7.03	3.3	6.23	12.5	
Ge	14.41	16.8	14.41	16.8	8.8	90.6	18	200	4.36	4.5	14	
Sn	49.55	37.04	49.55	37.04	37.03	57.23	23.45	31.06	19.8	17.09	19.78	

the exception of two sample (pegmatitic neosome) which falls within the metaluminous (Fig. 4) this is due to its alkali elements.

L-P = Low peraluminous; m-P – moderate peraluminous; h-P – high peraluminous and f-P felsic peraluminous.

Frost et al. (2001) classification scheme that is composed of three indexes (Fig.5):

Fe-number -Fe-number is calculated as weight proportion of feot/(feot+mgo). Frost et al. (2001) proposed the terms “ferroan” for rocks where the Fe is more abundant than Mg and “magnesian” for rocks were the Mg is more abundant than Fe. Mg is considered more abundant than Fe if the ratio feo/(feo+mgo) <0.5. all the rocks fall in ferroan domain, The Fe number determines whether the rocks are mainly magnesian or ferroan and this provides a clue on the differentiation history of granitic magma. The Fe enrichment used to distinguish between granitoids from different tectonic environment.

Modified alkali-lime index is expressed by the composition and abundance of feldspar or other minerals containing K and Na relatively to the silica content. It can be divided into calcic, calc-alkalic, alkali-calcic and alkali fields (Frost et al., 2001).

Aluminium Saturation Index (ASI) A = NK versus ASI diagram, where A/NK stands for molecular Al_2O_3/(Na_2O + K_2O) and ASI for molecular Al_2O_3/(Na_2O + K_2O + cao – 1,67*P_2O_5). In fact, it is the A/CNK parameter of Shand (1943), corrected for the Ca content in apatite.

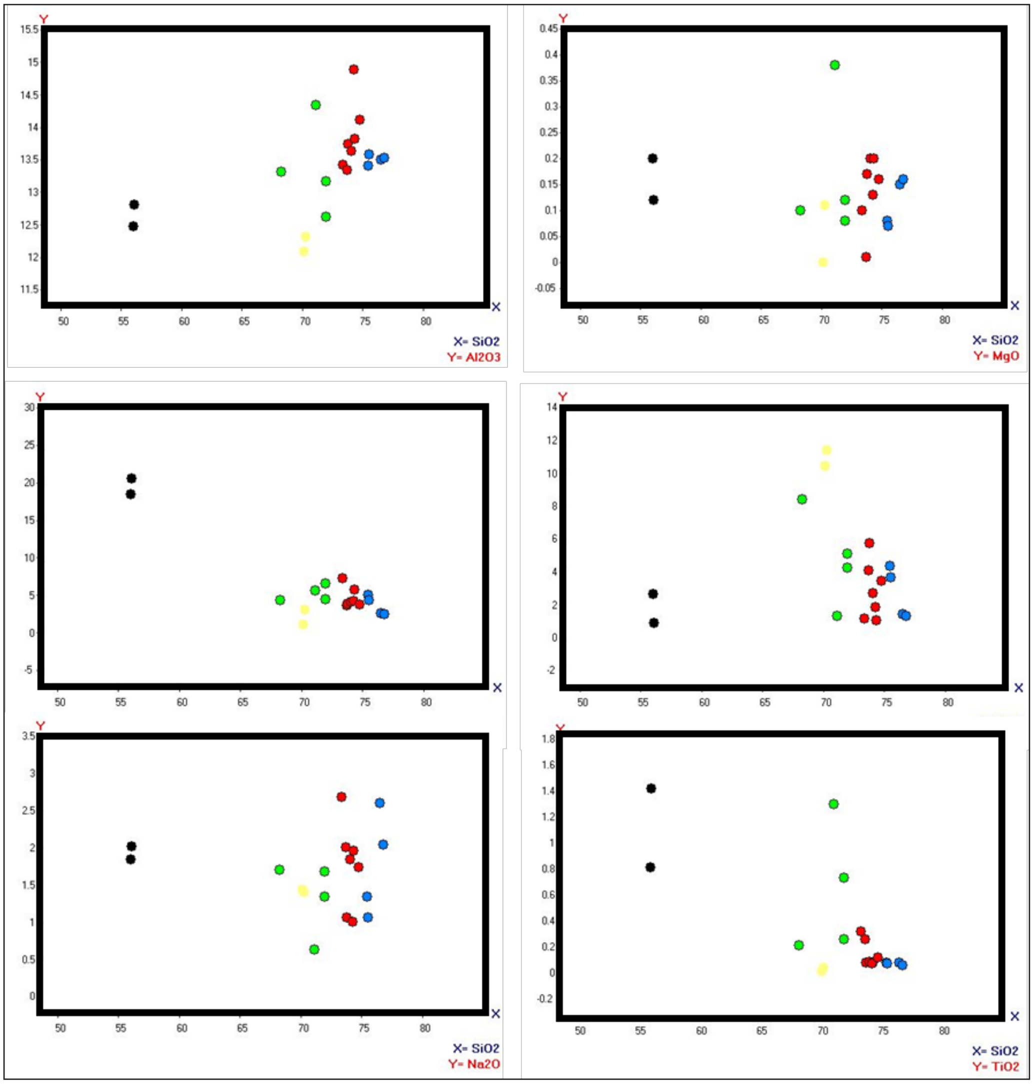

Figure 3. Variation diagrams (a–f) of the major element against silica (Harker).

ASI makes the chemical discriminant between peraluminous granitoids (ASI > 1) and metaluminous granitoids (ASI < 1). The peraluminous granitoids have more aluminum that can be accumulated in the feldspars and must have another aluminum phase present. The pegmatitic neosome plots within the pera-alkaline due to the low aluminum accommodated with the feldspar while the metatexite falls to be peraluminous in nature (Fig. 5a–c).

3.6. Tectonic discrimination

Tectonic discrimination diagrams are diagrams used to distinguish magma that are produced in different tectonic environment based on their chemical composition (Batchelor and Bowden, 1985, and Pearce et al., 1984). The essence of this chemical data is to distinguish the geodynamic content of granitic rock emplacement. In particular, anatectic granite is usually a function of protolith rock composition and of melt crystallization history being the tectonic environment (Rollinson, 1993 and Frost et al., 2001). Pearce et al. (1984) distinguished four types of tectonic environment Ocean Ridge Granites- Granite of oceanic ridge, fore-arc and back-arc; Volcanic Arc Granites- Oceanic volcanic arc and active margins granite; Within Plate Granites- Intraplate granites in attenuated crust and island arc; Collisional Granites- Collisional granites, syn-tectonic associated with continental-continental collision and continent arc. When plotted all the rocks fall in. The diagram of Batchelor and Bowden (1985) which is based on major element where be distinguished between granite formed from mantle fractionate, pre-orogenic granite, post-collisional uplift granite; late orogenic granite, anorogenic granite, syn-collisional granite and post-orogenic granite.

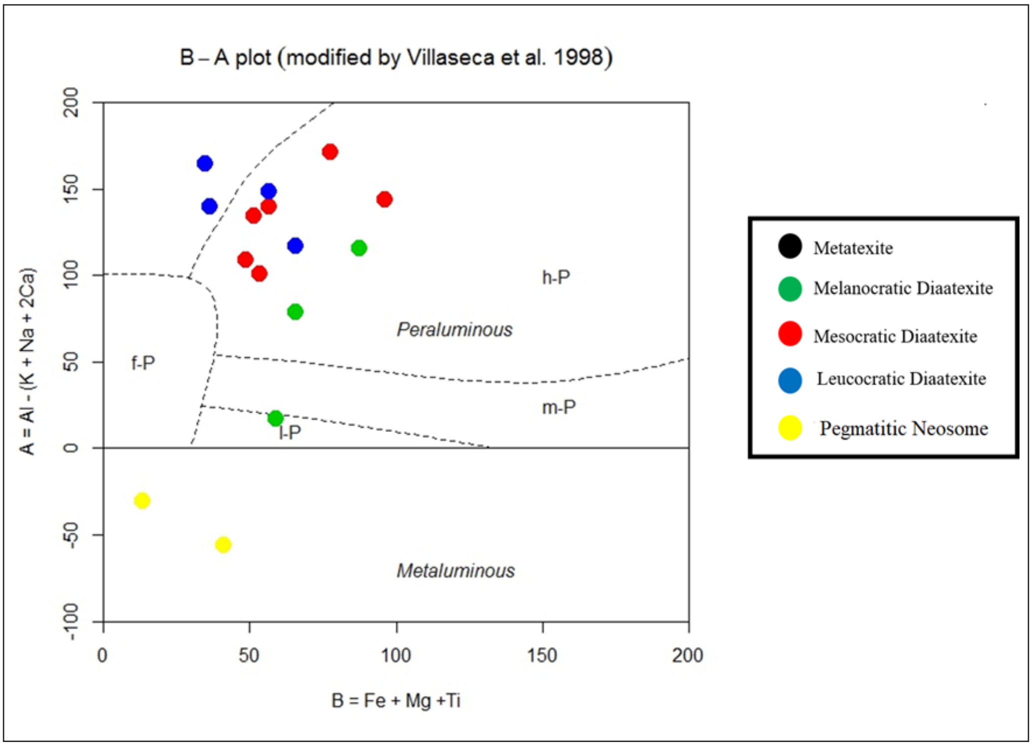

Figure 4. B-A diagram proposed by Debon and Le Fort (1983) modified after Villaseca et al. (1998) with fields for various peraluminous rock types.

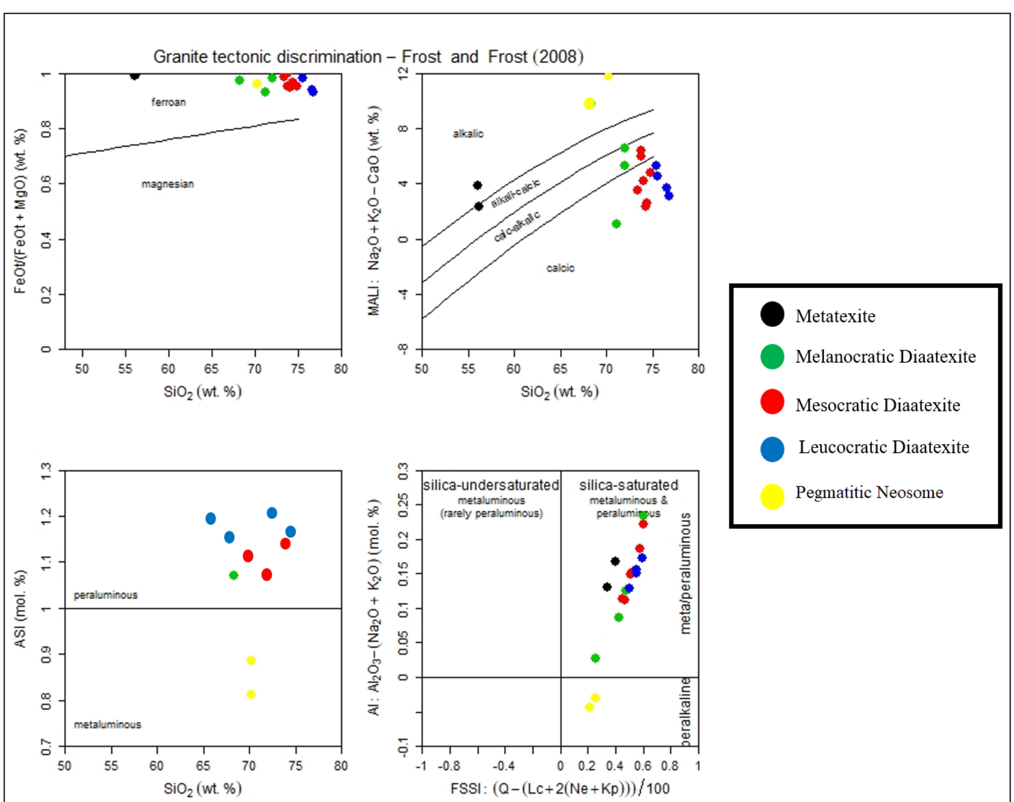

Figure 5. Frost et al. (2001) classification scheme.

The pegmatitic neosome granite fall in the anorogenic domain, (Figs. 6 and 7).

4. Discussion

Field observation has revealed that the major lithologic unit metatexite, diatexite (Melanocratic, Mesocratic and Leucocratic Diatexite. The morphologies vary in texture and composition and comprise; fine, medium to coarse grained in hand specimen mineral grained description. The gradational contact relationships between the various morphologies suggest each lithologic to come from the same parental source and shows a level of metamorphic transformation rather not emplacement process of another magmatic bodies. Petrographic studies have shown that the migmatite morphologies are granitic in composition and consist mainly of quartz, feldspar, hornblende, biotite and sillimanite, corderite, garnet, orthopyroxene as metamorphic minerals. Almost all the quartz in the rocks show wavy extinction and the feldspar twinning are almost completely obliterated due to the effect of stress (metamorphism) (Plates 1,2,4, and 6–8). The presence of Myrmekite in the rock is evidence of tectonic deformation. Major elements composition has revealed that the rock is peraluminous and has calc-alkaline affinity. TiO_2 versus SiO_2 discrimination, SiO_2 versus $Al_2O_3/(CaO + Na_2O + K_2O)$ diagram, and Ternary diagram of $Al_2O_3/(FeOT + MgO)$-3CaO-5(K_2O/Na_2O) on which the composition of plotted. has shown that the rock is a paragneiss (was derived from metasedimentary source with the exception of pegmatitic neosome which has an orthogneiss origin). Ferre and Caby (2006), concluded that the in area have S-type characteristics. These authors have apparently drawn this conclusion that the migmatite morphologies are exclusively peraluminous. Major element composition has shown that the granites are ferroans, [have Iron number (Fe#) ranging from 0.86 to 0.98], mainly more calcic to alkalic (as shown on the Na_2O+K_2O-CaO *vs.* SiO_2 discrimination diagram (Fig. 5). Ferroan magmatism is a characteristic feature of the Proterozoic eon. The end products of this magmatism are feldspathic rocks that are extremely enriched in FeO relative to MgO (FeO/(FeO + MgO) > 0.8) (Frost and Frost, 2008). Frost and Frost (2008) acknowledged that partial melting of tonalitic to granodioritic crustal rocks at low pressure can produce slightly peraluminous high-silica, ferroan, calc-alkalic melts which the rock in the area obey this conclusion (Fig. 5)

Petrographic study reveals that the modal composition of ferromagnesian mineral (biotite) and plagioclase decreases from the Metatexite to Leucocratic diatexite vis versa increase of orthoclase and orthopyroxene. This suggests that metamorphic crystallization dominated by fractioning of plagioclase and biotite has played a significant role in the evolution of the migmatite morphologies. The decrease in the concentration of FeOt, MgO Al_2O_3 and CaO with increasing acidity (SiO_2) supports the earlier observation. The negative correlations between CaO, P_2O_5, MgO, FeOt, MnO, TiO_2 and SiO_2 suggest resulted from metamorphic crystallization during migmatitic rocks transformation. The variation trends of most of the major and trace elements (Fig. 3–f) in the migmatites morphologies show a differentiation process such as partial melting, magma mixing, restite unmixing or metamorphic crystallization (Ferre et al., 1998).

4.1. Possible source rock/tectonic origin

The peraluminous nature of the, particularly the less evolved members precludes an origin from the melting of a strongly peraluminous sedimentary protolith. This character requires a peraluminous protolith of sedimentary sources (Ferre et al., 1998).

In conclusion, it could be deduced that the S-type signature (Fig. 5) of the rocks have originated from partial melting of crustal protolith with change in composition in a deforming activity.

Considering the geochemical and petrographically and morphological characteristics of the rocks, numerous studies indicated that trace elements can be used to discriminate between different tectonic setting of granitoid magmas (Pearce et al., 1984) (Fig. 6). However, they must be used with caution as they could represent the formation of the protolith rather than those derived from magma. Pearce et al. (1984) suggest a set of diagrams using high field strength elements such as Zr, Ta, Y, that are most stable under various conditions and hydrothermal metamorphism (Fig. 6). Batchelor and Bowden (1985) proposed a tectonic discrimination environment considering the parameter of R1& R2 where R1 stands for 4Si-11(Na+K)–2(Fe+Ti), R2 stands for 6Ca+2Mg+Al (Fig. 7) which is based on major element where he distinguished between granite formed from mantle fractionate, pre-orogenic granite, post-collisional uplift granite; late orogenic granite, an-orogenic granite, syn-collisional granite and post-orogenic granite. The rock in the study area falls within the syn-collisional, volcanic Arc Granitoids which deduced that the rocks have been formed from/through partial melting of clastic sediments that are very common in the continental crust with the exception of the pegmatitic neosome which is

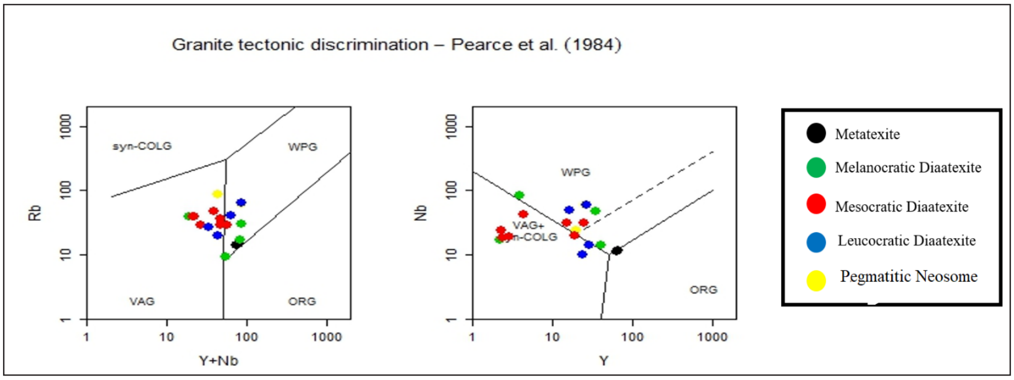

Figure 6. Discrimination diagram for geotectonic environment by Pearce et al. (1984). Abbreviation: ORG - Ocean Ridge Granites; VAG - Volcanic Arc Granites; WPG - Within Plate Granites; syn-COLG - syn-Collisional Granites

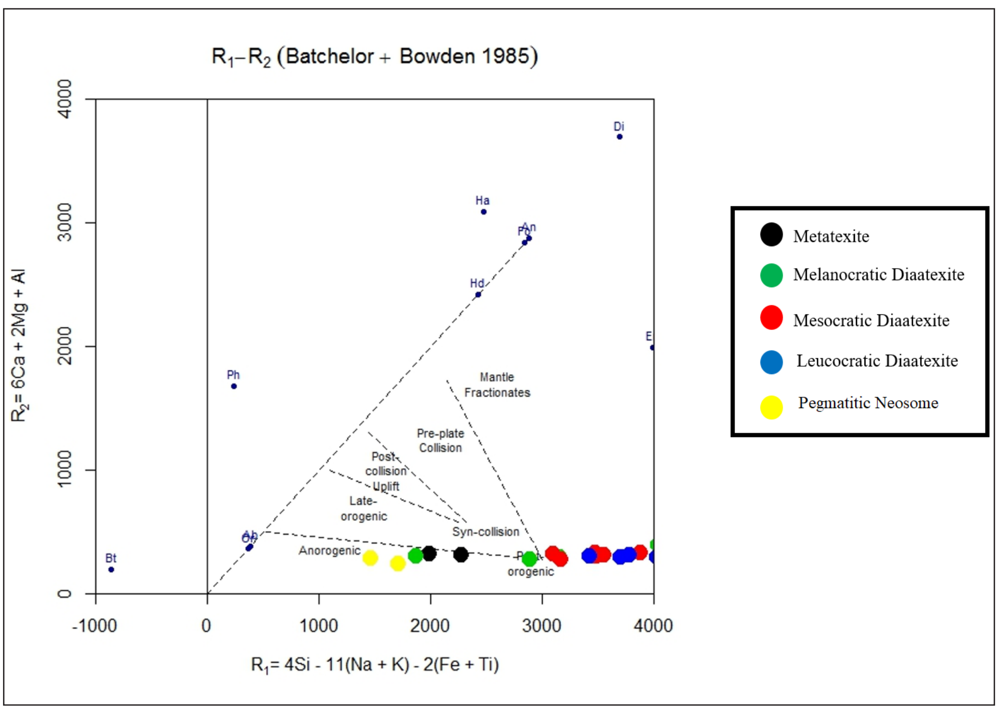

Figure 7. Batchelor and Bowden (1985) discrimination diagram, which distinguishes between granites from fractional mantle, pre-orogenic granites, post-collisional uplift granites, late-orogenic granites, anorogenic granites, syn-collisional granites and post-orogenic granites.

anorogenic (Fig. 7) which may be due to activities of foreign material.

5. Conclusion

The study area comprises of metatexites, diatexites, as its rock types. The granite suites vary in texture and composition. Field, morphological, petrographic observations combined with geochemical data show a genetic relationship between the metatexites, diatexites to be of the same source but showing different structural, chemical and textural transformation. Petrographic studies revealed that quartz; orthoclase, plagioclase, sillimanite, orthopyroxene and biotite constitute the major minerals present in the rocks, while apatite, ilmenite, rutile and zircon are the accessory minerals present in the rocks.

Geochemical studies have shown that the rocks are ferroan to magnesian, highly peraluminous, have calcic affinities-collisional S-type granites derived through partial melting of crustal rocks and are paragneiss (derived from sedimentary / metasedimentary source).

The high SiO_2 ($Na_2O + K_2O$) and Al_2O_3, MgO, Fe_2O_3 & CaO low concentration imply that the primary magma was derived from partial melting that involves lower crust. The compositional trends of the rocks indicate a decrease Al_2O_3, Fe_2O_6, MgO, CaO, TiO_2 with increasing SiO_2 which might be due to the fractionation of plagioclase or biotite or crustal contamination of magma during partial melting.

References

Ajibade AC, Fitches JB. Togo-Benin-Nigeria shield: evidence of crustal aggregation in the Pan-African belt. Tectonophysics 1988; 165:125–9.

Ajibade AC, Rahaman MA. Proterozoic crustal development in the Pan-African regime of Nigeria. Amer Geophys Union 1988; 4: 259–71.

Batchelor RA, Bowden P. Petrogenetic interpretation of granitoid rock series using multicationic parameters. Chem Geol 1985; 48:43–55.

Collins WJ, Beams SD, White AJR, Chappell BW. Nature and origin of A-type granites with particular reference to southeastern Australia. Contri Mineral Petrol 1982; 8:89–20.

Debon F, Le Fort P. A chemical–mineralogical classification of common plutonic rocks and associations. Transactions of the royal society of Edinburgh. J Earth Sci 1983; 73:135–49.

Ferre EC, Caby R. Granulite facie metamorphism and charnockite plutonism: example from the neoprotorozoic belt of Northern Nigeria. Lithos 2006; 12(11):1–8.

Ferre EC, Caby R, Peucat JJ, Capdevila R, Monie P. Pan-African, post-collisional, Ferro-Potassic granite and quartz-monzonite plutons of Eastern Nigeria. Lithos 1998; 45:255–79.

Frost BR, Barnes CG, Collins WJ, Arculus RJ, Ellis DJ, Frost CD. A geochemical classification for granitic rocks. J Petrol 2001; 42:2033–48.

Frost BR, Frost CG. On ferroan (A-Type) granitoids: their compositional variability and modes of origin. J Petrol 2008; 52:39–53.

Hirsh H, Coen MH, Mozer MC, Hasha R, Flanagan JL. Room service, AI-style. IEEE Intell Syst 2002; 14(2):8–19.

Jibrin AI, Aliyu M, Lawal A, Haruna AI. Kariya II, Yelwa HM. The pre-cambrian rocks of North- Eastern Nigeria. Sci Forum (J Pure Appl Sci) 2018; 18:1–6.

Jibrin AI, Haruna AI, Maigari AS, Lawal A, Umar US, Abdulmumin Y, et al. Morphology, petrology and geochemistry of Pan African migmatites around Liman Katagum and Bagel North- East Nigeria. Sci Forum (J Pure Appl Sci) 2021; 21(2):352–6.

Pearce JA, Harris NWB, Tindle AG. Trace element discrimination diagram for the tectonic interpretation of granitic rocks. J Petrol 1984; 25:956–83.

Rollinson H. Using geochemical data: evaluation, presentation, interpretation. Longman Group UK Limited, Harlow, UK, 1993.

Villaseca C, Barbero L, Herreros V. A re-examination of the typology of peraluminous granite types in intracontinental orogenic belts. Transactions of the royal society of Edinburgh. Earth Sci 1998; 89:113–9.

Wright EP. Basement complex. The geology of the Jos Plateau. Geol Survey Niger Bull 1985; 1:12–47.

Wright JB, Currie KL, Chappell BW. A-types granites: geochemical characteristics, discrimination and petrogenesis. Contrib Mineral Petrol 1985; 95:407–19.